

# FODA/IBEA-TDMA: A FLEXIBLE FADE COUNTERMEASURE SYSTEM FOR INTEGRATED SERVICES IN USER ORIENTED NETWORKS

Celandroni N.\* , Ferro E.\* , James N.+ , Potortì F.#

\***CNUCE**, Institute of National Research Council

Via S. Maria 36 - 56126 Pisa - Italy

Phone: +39-50-593207/593312

Fax: +30-50-589354 - Telex: 500371

+ **GEC-MARCONI** Research Centre- Great Baddow-UK

Marconi Research Labs., West Hanningfield Road, Graet Baddow,  
Chelmsford, Essex CM2 8HN, U.K.

# **Telespazio** S.p.A. Scholarship holder at CNUCE

## Summary

A flexible, processor based, TDMA station has been implemented. This station and its associated variable data rate modem enables users to implement very complex frame structures under software control. Burst rates of 512 Kbit/s - 8.192 Mbit/s and different coding rates are possible allowing the transmitted bit energy from each station in the network to be adapted to prevailing conditions. The proposed application of the station is the transmission of mixed stream and packet traffic, in a LANs interconnection via satellite environment, using a modification of the FODA<sup>5</sup> technique. The association of the up-link power control feature with the bit and coding rate variation gives the system an interesting ability to cope with fade conditions. The link outage probability is investigated for the Olympus transponder in Ka band. The ability of the system, together with the good performance of Olympus, shows that the Ka band is usable for the above mentioned types of networks without prohibitive fade degradation, at least for limited coverages.

**KEYWORDS** TDMA controller · Variable bit rate modem · Fade countermeasure · Outage  
Multiple access · Satellite network

## Introduction

A TDMA station has been developed for use in a number of advanced communications experiments. The station, which consists of a processor based TDMA controller and a digitally-implemented multi-rate modem, allows individual data packets to be transmitted at bit rates in the range 512-8192kbit/s. Each packet can also be protected by variable rate FEC coding independently of other packets within the burst.

The station has the following major features:

- Flexibility** Only those functions which would be too slow or too inefficient to implement in software are implemented using hardware. Many different TDMA systems can thus be implemented with no hardware modification.
- Adaptability** The controller hardware allows the content of the TDMA frame to be changed on a frame-by-frame basis under software control. It also allows variable FEC coding and symbol rates to be applied to specified parts of each burst. In

addition, to allow complete flexibility of data formatting, the modem has been designed to accommodate changes of symbol rate *within* each data burst.

**Expandability** The controller is based on the industry standard VMEbus architecture so that additional hardware functions can be added easily if required.

The hardware consists of two controller units (one transmit and one receive) and a burst mode modem. Figure 1 is a photograph showing the transmit controller (bottom) and the receive controller (top). The *core software* is a firmware package which implements a basic TDMA system on this hardware. This firmware enables a user to set up a wide range of frame structures and network types and it can demonstrate and utilise all the basic features of the hardware. Advanced TDMA systems, which fully utilise the flexibility and adaptability of the hardware, can be implemented by writing additional software.



Figure 1. The TDMA controller hardware

Part I of this paper contains a brief description of the TDMA station in terms of the architecture both of the hardware and of the core software. Part II describes a more advanced system which uses additional software in order to allow the TDMA station to operate with both packet and stream data.

## Part I - The TDMA station

### 1.1 Controller architecture

The TDMA controller is implemented using two VMEbus based racks, one for the transmit controller and one for the receive controller. High speed communication between the two controllers is possible using a SCSI bus. The controller is based on a proprietary Motorola 68030 processor card containing 4Mbyte of RAM. This CPU communicates over the VMEbus with a number of other cards. Figure 2 is a block diagram of the controller hardware.

This hardware allows users to implement a wide range of TDMA systems in software but it does impose some restrictions. These were necessary since, in some cases, the software would be unable to react quickly enough to external events.

- Each burst must start with a carrier and bit-timing recovery sequence (CBTRS). This is actually a restriction of the modem.
- The frame must include a reference burst (RB) containing the master unique word (MUW). The MUW maintains synchronisation of the receive hardware frame counter. Apart from the MUW the remaining content of the RB is unimportant to the hardware. Only one MUW must appear in each frame. The maximum frame length is 64ms.
- Each data burst must consist of a control sub-burst (CSB) followed by a number, possibly zero, of data sub-bursts (DSBs). The CSB is decoded by the hardware and provides information necessary for the reception of the following DSBs.

In the transmit controller data is received from a number of terrestrial interfaces. A transmit serial interface card provides stream interfaces at 64kbit/s (G.703) and 384kbit/s (RS449), The CPU card provides an Ethernet interface and other LAN interfaces can be provided by purchasing proprietary VME cards. Data collected from the terrestrial interfaces is formatted in to the appropriate bursts by the CPU. The transmit modem interface card then controls data transfer to the modem.

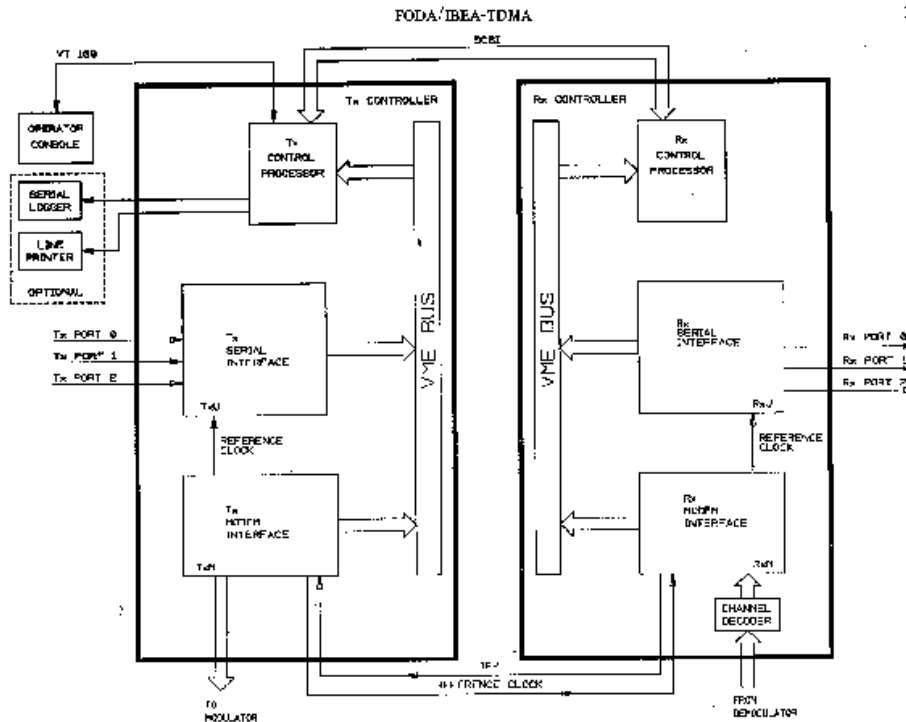


Figure 2. TDMA controller block diagram

The precise time at which individual bursts are sent to the modulator is determined by the transmit event memory (TEM). This consists of two memory arrays organised in a ping-pong arrangement, each capable of storing up to 512 events. During one frame the software can update one side of the TEM whilst the other side is being used by the hardware. The software originated events are then used by the hardware in the subsequent frame. Each event within the event memory contains an 18 bit time code, which defines the time at which a particular action will take place (in 244ns ticks from the start of transmit frame), and a 14 bit function code. The transmit events are used, amongst other things, to open and close the burst gate and to set the modulator output level. A special function code can be used to define the end of the transmit frame by providing a reset pulse to the transmit frame counter.

When the transmit burst gate is open, formatted data is sent from the CPU to the transmit modem interface under interrupt control. This data is then convolutionally encoded and scrambled if necessary. The code rates available are all based on a standard 1/2 rate convolutional code but puncturing logic allows additional code rates of 2/3 and 4/5. The hardware appends the necessary tail bits to flush the decoder at the receive side and will, if required, append a short CRC to each transmitted DSB.

In the receive controller 4 bit soft-decision data received from the demodulator is passed to the convolutional decoder where it is decoded if required using the Viterbi algorithm. The receive hardware also provides a measurement of the estimated channel quality for each DSB by monitoring the recovered data soft decisions. The hardware simply observes the occurrence of particular soft decision levels and accumulates these over a sub-burst. This count is then made available to the software. Assuming a Gaussian distribution an approximation to the short-term BER can then be computed. This method is much faster than counting errors in the UW and it provides a channel estimate which can be used in adaptive fade countermeasures (FCM) algorithms.

The decoded data stream is then routed to the receive modem interface. This interface uses a receive event memory (REM) to allow real-time reception and decoding of the received bursts. The REM is identical in structure to the TEM. The receive function code contains information on, amongst other things, the initial code rate and symbol rate of the bursts within the frame. A special function code can be used to generate a transmit frame pulse which will reset the event counter on the transmit controller. This is used by slave stations to synchronise their transmit frame to that of the master.

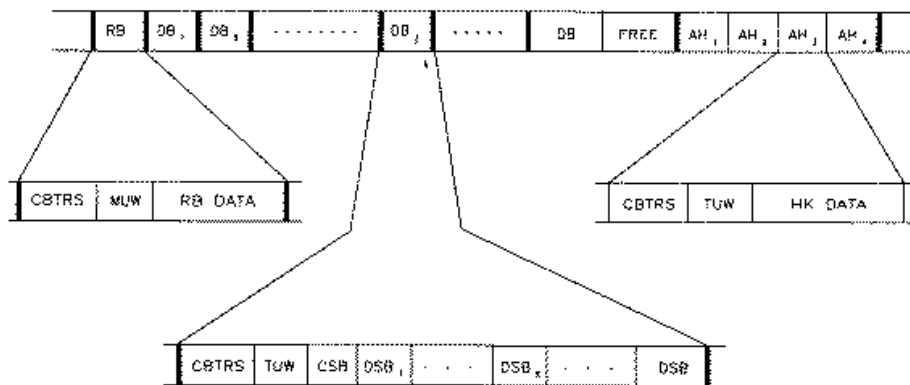


Figure 3. Typical frame structure

Three unique words are used by the hardware. The master unique word (MUW) is reserved for use in the reference burst only. Receipt of the MUW by the hardware resets the receive frame counter and thus marks the start of the receive frame. The second type of unique word is the traffic unique word (TUW) which is used by all bursts other than the reference burst. Finally, the sub-burst unique word (SBUW) is used at the start of each data sub-burst. Each of the three unique words is composed of the same basic programmable pattern and its complement ( $UW$  and  $\overline{UW}$ ). The SBUW uses the basic  $UW$  pattern whilst the MUW and TUW use  $UW$  followed by either  $UW$  or  $\overline{UW}$ . The receive hardware accommodates two, software selectable, thresholds for unique word detection. In addition to their synchronisation functions the unique words are used by the hardware for data ambiguity resolution and to reset the optional de-scrambler to its start-up vector.

When a data burst (DB) is received the hardware decodes the control words contained within the CSB and uses them to drive the receiver during the reception of subsequent DSBs. This allows each DSB to have its own particular parameters. The hardware decoding of the information in the CSB is

required since software would not be fast enough. It does, however, introduce a slight restriction on the formatting of the data burst.

The decoded and descrambled data is then passed to the software under interrupt control along with a number of status words which provide information about the received data. The CPU can then route data to the stream outputs implemented by the receive serial interface or to any other output interface available.

Figure 3 shows a typical frame structure for this TDMA station as implemented by the core software. The RB and DB have been described already and their format is partly determined by the hardware. In order to maintain slave synchronisation in the network, the frame also contains a number of reserved slots which are used for short acquisition bursts. These convey information about slave timing to the master.

The core software also provides an extensive menu driven interface to users via the controller console. This menu system allows the user to adjust all of the variable parameters of the system. It also provides a powerful monitoring facility by displaying real-time status information on various display screens.

### 1.2 The burst-mode modem

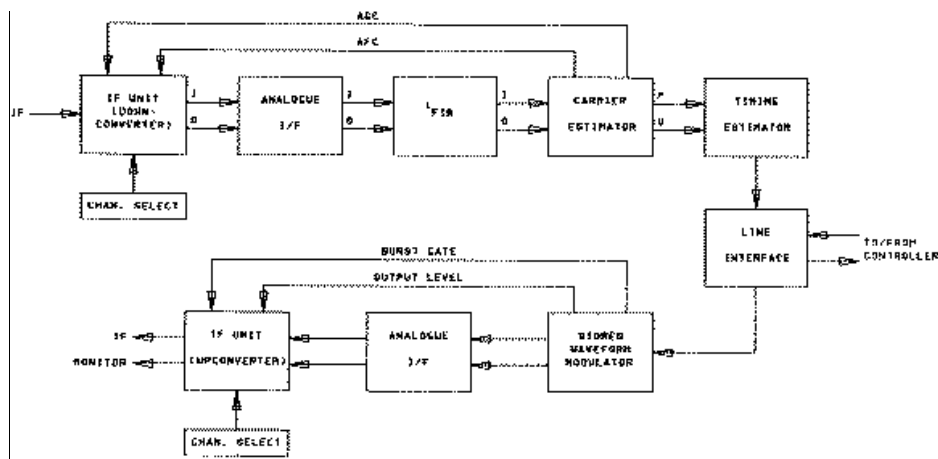


Fig. 4. Modem block diagram

A special feature of the modem is that it is capable of dynamically adjusting its transmission rate within a data burst. This allows the individual DSBs of a DB to have different symbol rates (and, hence, different energies) as required. The symbol rates available are 512, 1024, 2048 and 4096 kbaud using either BPSK or QPSK modulation formats. A bit rate range of 512-8192 kbit/s is thus available to the system. In order to achieve the variable symbol rate requirements the modem, a block diagram of which is shown in figure 4, is implemented using digital signal processing (DSP) techniques.

#### 1.2.1 Stored waveform modulator

In an ideal modulator positive and negative impulses representing the two data states of the incoming binary data sequence are passed through a filter with a Nyquist frequency response. Digitally this is equivalent to the convolution:

$$F(i) = \sum_{j=-\infty}^{+\infty} I(i-j)C(j)$$

where  $I(n)$  is the  $n^{\text{th}}$  data impulse ( $\pm 1$  depending on the data state),  $C(n)$  is the  $n^{\text{th}}$  filter coefficient and  $F(n)$  is the  $n^{\text{th}}$  output sample. This function is implemented using a Finite Impulse Response (FIR) filter.

As a consequence of Nyquist's sampling theorem the output of the digital modulator has aliases at the sampling frequency which must be removed by analogue anti-alias filters (AAFs) before transmission. Since the above convolution has only one output sample per data symbol it leads to serious AAF implementation problems because the aliases are at a low frequency with respect to the wanted spectrum. This problem is overcome by increasing the input sampling rate by placing intermediate zero value samples in the input stream. In this way it is possible to obtain output sampling rates which are integer multiples of the data rate. Interpolation by a factor of four for instance would shift the aliases to four times their original frequency so that they become much easier to remove by analogue filtering. Symbol rate changes can conveniently be effected by changing the interpolation rate. In this way the output sampling rate, and consequently, the alias frequency, remains constant. The TDMA burst modulator has a fixed sampling clock of 16.384MHz. Interpolation rates of 4, 8, 16 and 32 thus provide the required transmission rates of 4096, 2048, 1024 and 512 kbaud respectively.

The interpolated FIR can be implemented relatively simply by using a *stored waveform modulator* structure. The output results for all possible input sequences are pre-computed and stored in a Read Only Memory (ROM). This acts as a large look-up table which is addressed by the past  $n$  symbols of the incoming data sequence and an interpolation count. The resulting output sample is then available for transfer to the DAC.

### 1.2.2 Demodulator

In the demodulator the received signal, polluted by noise and other effects, is first downconverted to two quadrature baseband signals by an IF converter. Following anti-alias filtering the signals are sampled by two Analogue to Digital Converters (ADCs) and the resulting complex sequence is passed to the digital processor. The complex samples are then filtered by a FIR filter, the response of which is selected depending on the expected burst symbol rate.

Once the received sample sequence has been filtered the original data stream must be extracted. In order to do this the demodulator must make estimates of several parameters from the received, noisy signal. For a phase modulation such as QPSK the parameters of interest are:

- $\omega$  An unknown carrier frequency translation (due to oscillator inaccuracy in the satellite and the earth stations).
- $\phi$  An unknown carrier phase shift (modulo  $2\pi$ ).
- $\tau$  An unknown timing phase shift (modulo  $T$ ).

The carrier frequency error consists of two components. The downlink frequency error  $\omega_d$  is due to the satellite frequency conversion error and the downconverter in the local receive station. This error can be up to  $\pm 40$ kHz but it applies to all of the bursts in the frame. The demodulator removes this by an initial AFC sweep at the start of operation and tracks the slow variations thereafter. The uplink frequency error  $\omega_u$  is more of a problem. It is caused by the variations in transmit frequency at the remote stations and is thus different for each burst in the frame. In a typical system  $\omega_u$  can be of the order of  $\pm 4$ kHz. The value of  $\omega_u$  must be estimated very rapidly at the start of each burst.

In order to allow parameter estimation, and thus data demodulation, before the arrival of the UW, each burst is preceded by a short preamble. The parameters  $\omega_u$  and  $\phi$  are estimated simultaneously at the start of each burst using the unmodulated carrier preamble. Two types of estimator were considered. The *feedback* estimator makes an estimate of the error between the wanted phase and  $\phi$  and adjusts the incoming phase to minimise the error. The *feedforward* estimator makes absolute estimates of  $\phi$  and then passes these forward to a later stage where an appropriate correction is made. The feedback estimator works well under low signal-to-noise conditions and can accommodate large

frequency errors, however, in a burst mode system, it does have a major problem called *hangup*. This phenomenon leads to occasional very long acquisition times when the initial phase error is close to  $\pi$ . This is not acceptable for a burst-mode system where reliable acquisition in a limited time is necessary. The feedforward system does not suffer from hangup but, unfortunately, it is not particularly suited to situations where the initial frequency offset is large. In order to overcome these problems this modem uses two digitally-implemented feedback estimators which are initialised to different states just prior to the expected reception of a burst. Since the initial phase of each estimator is different they cannot both suffer from hangup and so one will always acquire within the time available.

The symbol phase,  $\tau$ , is estimated using the reversals present at the end of the preamble. Several estimators matched to different clock phases are used and the phase giving the largest output is used to initialise the clock tracking loop. Once the symbol phase has been estimated the demodulated data is available to the receive controller.

## Part II. The FODA/IBEA system

The presented application of the described above hardware consists of a user oriented satellite network interconnecting a number of LANs, placed at different sites. At each site, a moderated small earth station consisting of a 2-3 m dish and an HPA of 10-100 W is installed at the user premises and is connected to the satellite controllers through the modem. The employed payload is that of any geostationary satellite, working in the  $K_u$  or  $K_a$  bands with a global coverage. The inter LAN packetized traffic is concentrated at each site on a satellite router which is connected to the controller and to one or more LANs (figure 5).

The traffic produced by the various applications disseminated over the LANs may be either isochronous (stream) or anisochronous (datagram). Typical stream applications are: telephony, videotelephony, tele-education and videoconference, while all of the classical EDP applications are substantially of datagram type.

The satellite access scheme, running on the controllers, is a TDMA system based on demand assignment of the channel capacity. The system is able to guarantee the bandwidth requested by the stream applications with a limited packet jitter, while doing its best to reduce the queuing delay of the datagram packets. Two priority classes are provided for datagram traffic, allowing a lower delay for interactive traffic with respect to bulk traffic. For all the types of traffic the system offers the data quality requested by the applications and specified in the class of service (COS) parameter. Care must be taken in choosing the type and implementation of the LAN to be crossed by the stream data. Indeed, stream applications are jitter sensitive and some of them, such as telephony (CCITT rec. G.114), are also delay sensitive. The LANs must therefore guarantee, within certain tolerances, the bandwidth requested by the applications. Contention based LANs, such as Ethernet, are generally unsuitable to carry stream traffic. However, if the peak of the total load is kept below a limited fraction of the network capacity, the introduced jitter can be acceptable<sup>7</sup>. The jitter accumulated during the internetworking system crossing can be removed by the destination application, using an *elastic buffer*, at the cost of an additional end-to-end delay. Bulk traffic is much less sensitive than stream to jitter and delay, while the delay caused by the satellite network crossing penalises but still allows interactive applications.

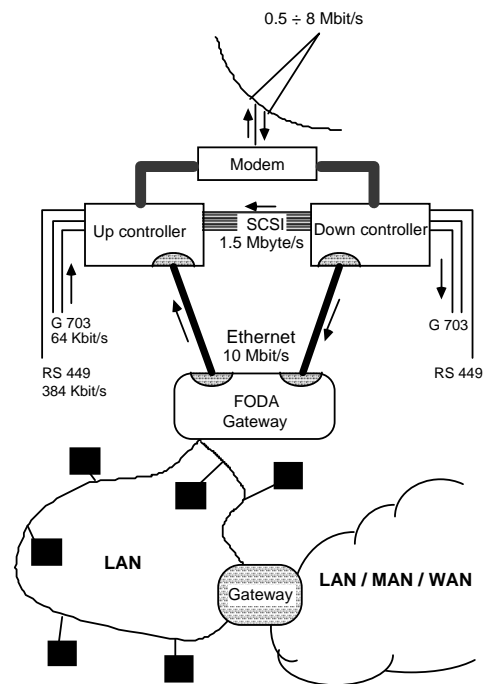


Fig. 5 - The environment

The name of the access scheme is FODA/IBEA (FIFO Ordered Demand Assignment/Information Bit Energy Adaptive). The first part of the name is the same of a system previously realised at fixed bit and coding rates<sup>5</sup> because the adopted mechanism for capacity request and assignment of datagram is substantially the same. The second part indicates that the energy contained in an information bit can be increased to achieve the application requested data quality under unfavourable transmitting/receiving conditions (signal fading and/or smaller earth station performance). The information bit energy is changed by varying the up-link power, when possible, or gradually varying first the coding rate and then the burst transmission bit rate. Some ideas of the present system have been already anticipated<sup>1, 2</sup>.

## 2.1 The access scheme

The satellite controllers, the modem and the earth station are collectively called a *station*. Centralised control has been chosen because, while operating in fade conditions (high BER), a distributed system would cause frequent losses of synchronisation among the stations.

The control station, which can be selected from any of the user stations, is called a *master*. It sends a reference burst (RB) for frame synchronisation at the beginning of each 20 ms frame. The RB for frame  $n$  contains, in addition to other general information, the plan of the transmission time slots for the stations, valid for the frame  $n+1$ . The stream slots are allocated one per frame to the requesting stations up to a global amount (the *normal stream boundary*). When this boundary is reached, no further requests are accepted. The stream request (in bits/frame) is the resulting bandwidth needed by all the stream applications served by the station. The bandwidth of each stream allocation is maintained unchanged until a modification (or relinquish) request is sent by the requesting station. The remaining channel capacity is assigned to datagram services according to an algorithm described in reference 5, which cyclically assigns to each station a fraction of the relevant request. The datagram requests are computed by each station as the sum of two terms: one proportional to the volume of data present at the station in the datagram queue (the backlog), the other proportional to the incoming traffic rate. Denoting the backlog by  $B$  and the incoming traffic



rate by  $I$ , the datagram request is expressed as  $R = B + h I$  where  $h$  is a temporal constant. The simulation results of figure 6 and 7 are obtained by loading the channel with Poisson generators of datagram traffic for 10 stations. They show that the best value of  $h$  is 0.4s.

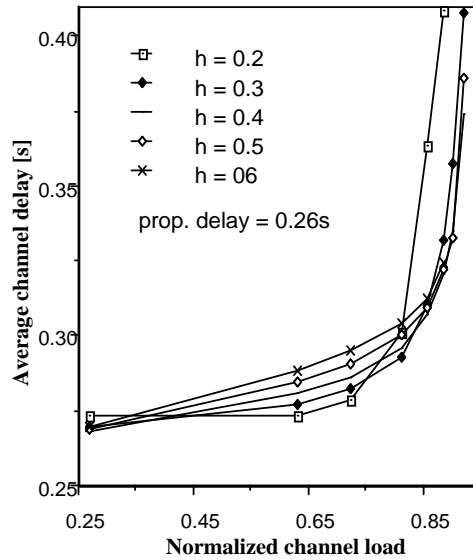


Fig. 6- End-to-end delay averaged over 30 s for various values of  $h$ .

Datagram and stream requests can be appended to existing data bursts or sent in pre-assigned control slots. Two control slots per frame are foreseen and they are assigned to the first two active stations having no data burst assignment in that frame, according to a round-robin scheduling algorithm.

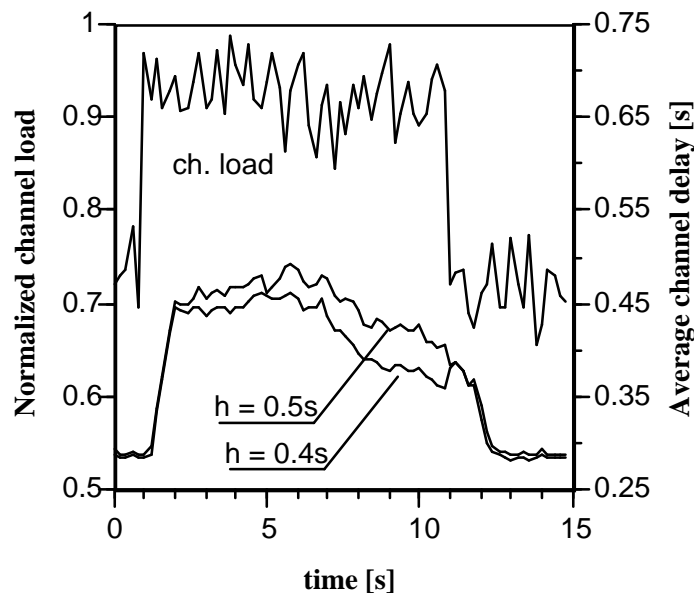


Fig. 7 - Channel delay averaged over 10 stations. Poisson datagram traffic. A step of traffic of 20% is applied to one station for 10 s.

A unique slot per station for both stream and datagram traffic is allocated in a frame. This choice induces a jitter in the receive times of the stream packets, because the size of datagram allocation varies in each frame. In order to reduce this jitter, the transmission of the stream packets received in a frame to the destination router can be optionally delayed up to the end of the receiving frame.

## 2.2 Behaviour in fade conditions

In Tab. 1 the transmission parameters (bit and coding rates) are reported, as function of the BER range relevant to the COS requested by the application, and of the  $C/N_0$  (carrier power to noise density ratio) available at the receiver. Four different classes of service are envisaged. As the chosen modulation scheme is QPSK, the bit rate is in the range 1-8 Mbit/s.

(a)-Class of service = 0 ( $BER < 10^{-8}$ )					
C/No range [dBHz]	Eb/No range [dB]	Fade range [dB]	Bit rate [Mbit/s]	Code rate	Data redundancy (+)
81	12	0	8	1	1
80.5 - 77	11.5 - 8	0.5 - 4	8	4/5	1.25
76.5 - 75	7.5 - 6	4.5 - 6	8	2/3	1.5
74.5 - 74	8.5 - 8	6.5 - 7	4	4/5	2.5
73.5 - 72	7.5 - 6	7.5 - 9	4	2/3	3
71.5 - 71	8.5 - 8	9.5 - 10	2	4/5	5
70.5 - 69	7.5 - 6	10.5 - 12	2	2/3	6
68.5 - 68	8.5 - 8	12.5 - 13	1	4/5	10
67.5 - 66	7.5 - 6	13.5 - 15	1	2/3	12

(b) - Class of service = 1 ( $10^{-8} < BER < 3 \times 10^{-7}$ )					
C/No range [dBHz]	Eb/No range [dB]	Fade range [dB]	Bit rate [Mbit/s]	Code rate	Data redundancy (+)
81 - 80.5	12 - 11.5	0 - 0.5	8	1	1
80. - 76.5	11 - 7.5	1 - 4.5	8	4/5	1.25
76. - 75	7 - 6	5 - 6	8	2/3	1.5
74.5 - 73.5	8.5 - 7.5	6.5- 7.5	4	4/5	2.5
73 - 72	7 - 6	8 - 9	4	2/3	3
71.5 - 70.5	8.5 - 7.5	9.5- 10.5	2	4/5	5
70 - 69	7 - 6	11 - 12	2	2/3	6
68.5 - 67.5	8.5 - 7.5	12.5- 13.5	1	4/5	10
67 - 66	7 - 6	14 - 15	1	2/3	12

(+) Data redundancy = (8/bit rate) x (1/code rate)

(c)- Class of service = 2 ( $3 \times 10^{-7} < \text{BER} < 3 \times 10^{-5}$ )					
C/No range [dBHz]	Eb/No range [dB]	Fade range [dB]	Bit rate [Mbit/s]	Code rate	Data redundancy (+)
81 - 78	12 - 9	0 - 3	8	1	1
77.5 - 75	8.5 - 6	3.5 - 6	8	4/5	1.25
74.5 - 72	8.5 - 6	6.5 - 9	4	4/5	2.5
71.5 - 69	8.5 - 6	9.5 - 12	2	4/5	5
68.5 - 66	8.5 - 6	12.5 - 15	1	4/5	10

(d) - Class of service = 3 ( $3 \times 10^{-6} < \text{BER} < 10^{-3}$ )					
C/No range [dBHz]	Eb/No range [dB]	Fade range [dB]	Bit rate [Mbit/s]	Code rate	Data redundancy (+)
81 - 76	12 - 7	0 - 5	8	1	1
75.5 - 75	6.5 - 6	5.5 - 6	8	4/5	1.25
74.5 - 73	8.5 - 7	6.5 - 8	4	1	2
72.5 - 72	6.5 - 6	8.5 - 9	4	4/5	2.5
71.5 - 70	8.5 - 7	9.5 - 11	2	1	4
69.5 - 69	6.5 - 6	11.5 - 12	2	4/5	5
68.5 - 67	8.5 - 7	12.5 - 14	1	1	8
66.5 - 66	6.5 - 6	14.5 - 15	1	4/5	10

Tab. 1 - Transmission characteristics for various classes of services

When the fade level changes on a link, the sending station updates the transmission parameters of the packets for each application that uses that link. The increase in data redundancy due to the decrease in  $C/N_0$  requires the assignment of wider transmission slots within the frame. The system reacts to a fade change in different ways for stream and for datagram.

For stream traffic the sending station computes the increased size of stream bandwidth and sends a modified stream request to the master. The master allows the crossing of the normal stream boundary because of the fade condition but rejects the request if the overall requested stream bandwidth exceeds another limit in the frame (the *high stream boundary*). The difference between the normal and the high stream boundary is the *common resource* that the system can use to support faded stream links. As in unfaded conditions the common resource is used by the datagram traffic, in faded conditions the channel capacity reserved for datagram is reduced. The high stream boundary can be set in any position between the normal stream boundary and the end of the frame. If it is set at the end of the frame, the capacity left for datagram may be occasionally used entirely for the stream allocations. The choice of the stream boundaries determines the ability of the system to cope with fade. This ability is substantially improved if the system is loaded with variable bandwidth applications such as videoconference traffic using a H.261 codec. Such applications can be requested to temporarily reduce their bandwidth when the fade conditions require it, i.e. when the entire common resource is still insufficient to accommodate the enlarged stream requests.

The system feature of supporting compressible applications strongly improves the outage probability for links with high capacity such as videoconference. This interesting feature is substantially a fade countermeasure based on a service-diversity. It allows the system to counter

fades even without employing any common resource, at the cost of some periods of time where the offered service is reduced in quality but still maintained. For example, in the H.261 videoconference, the video is degraded, but the voice quality is substantially unchanged when the bit rate is reduced.

The choice of the maximum bit rate of 8 Mbit/s was due to the necessity of limiting the cost of the stations. The other economic requirement of fully exploiting the transponder capacity imposes a multicarrier access to the transponder itself. Each carrier can be shared in TDMA, using FODA/IBEA or similar systems. The various systems may operate autonomously or may belong to a global MF-TDMA system as, for example, one of those presented in reference 4.

In order to limit the intermodulation interference due to multicarrier access, the satellite transponder HPA must be sufficiently backed-off. The IPFD (input power flux density) at the satellite must be kept constant and the transponder gain is set in such a way as to operate with the chosen back-off. In order to achieve that, the power level of the master is assumed as the reference level for all of the stations. Thus each station compares the levels of the bursts sent by itself with the level of the reference burst. The difference is used to modify the output power of the station's HPA.

Table 2 shows an example of link budget, using Olympus in  $K_a$  band<sup>14, 15</sup> and 2.5 m antennas equipped with a tracking feature. Three carriers are considered.

A C/T ratio due to intermodulation interference of -140 dBW/K has been assumed. This figure must be confirmed experimentally. In this example the up-link power control range is 12 dB. The value of the  $E_b/N_0$  ratio (12 dB) resulting from Table 2 is assumed as the reference unfaded value. It allows uncoded transmissions at 8 Mbit/s with a BER of  $10^{-8}$  for up-link fade conditions ranging from 0 dB (clear sky) to 12 dB.

Up-link freq. [GHz] (CH1)	28.072255	Total IPFD [dBW/n <sup>2</sup> ]	-101
Down-link freq. [GHz] (CH3)	19.475	Input Back-off [dB]	8
E/S EIRP [dBW]	73	Satellite EIRP [dBW]	55.5
E/S HPA Back-off [dB]	3	Output Back-off [dB]	4.5
Up-power Control Margin [dB]	12	E/S G/T [dB/K]	27.3
Satellite G/T [dBK]	14	Down-link C/No [dB]	90
C/T at satellite input [dBW/K]	-142.5	C/No at E/S receiver [dBHz]	83.2
Intermodulation C/T [dBW/K]	-140	$E_b/N_0$ at 8Mbit/s [dB]	14
Total Up-link C/T [dBW/K]	-145	Modem impl. margin [dB]	1
Up-link C/(No+I <sub>o</sub> ) [dBHz]	84.2	$E_b/N_0$ in clear sky conditions	12
Number of carriers	3	Link budget margin [dB]	1

Table 2. Link budget for the Olympus  $K_a$  transponder.

Three carriers at 8Mbit/s access the transponder in FDMA.

The 2.5 m E/S is equipped with a 70 W HPA.

Within the up-power-control (UPC) range each station can fully compensate the up-link fade level. The up-link residual attenuation due to out of range operation is compensated with adequate variable bit and coding rates (VBCR). The UPC range of each station depends on the station power margin. An interesting feature of the system is the freedom of sizing the stations according to the traffic intensity, the climatic conditions and the geographic location. Since the up-link  $C/N_0$  is less than that on the down-link (~6 dB), the system is particularly up-link sensitive, but this allows

stations of 58 dBW of EIRP to use the full capacity in unfaded conditions. For more powerful stations, such as the one reported in Table 2, the up-link sensitivity is well balanced by the UPC feature, which can absorb the first 12 dB of attenuation.

The high down-link  $C/N_0$  and the employment of the UPC are advantages offered by the very good performance of Olympus in terms of  $G/T$  and EIRP. These issues make the system able to react to low-to-medium attenuations without occupying a significant portion of the common resource (as will be shown later).

### 2.3 Link quality estimation and dissemination

Each sender station must know the  $C/N_0$  value available at the station to which its data is addressed, in order to choose the correct transmission parameters (bit and coding rates). The  $C/N_0$  is computed, given the bit rate  $r$ , as

$$\frac{C}{N_0} = r \frac{E_b}{N_0}$$

The estimation of  $E_b/N_0$  (bit energy to noise power density ratio) is made by each station, on each burst arrival, by detecting the percentage of bits whose magnitude is less than a certain threshold (fraction of the average signal amplitude). In figure 8 the probability that the signal magnitude is less than the threshold  $t$  is given.

Two different methods, a direct and an indirect one, may be followed for  $C/N_0$  information dissemination. By using the *direct method*, the  $C/N_0$  value is sent directly by each receiving station to each sending station. This method allows the maximum precision in the parameter estimation but it imposes a greater overhead due to the volume of control data requested. In fact, each station must frequently send an update of its fade condition to all the stations which are sending data to it. Moreover, if filtering and/or prediction techniques are employed to help estimate the  $C/N_0$ , each receiving station must process data relating to all the links it has with sending stations. In some cases this could be a large computing load.

With the indirect method it is supposed that each station broadcasts periodically only the  $C/N_0$  value relating to data it is receiving from the master. Let us call this quantity  $\zeta_{m-r}$ . The parameter  $\zeta_{s-r}$ , i.e.  $C/N_0$  available at the receiving station when the sending station is transmitting, results to be [6]:

$$\zeta_{s-r} = \zeta_{m-r} + C_{s-s} - C_{m-s}. \quad [\text{dB}]$$

where  $C_{s-s}$  is the carrier power level available at the sending station, when the sending station itself is transmitting and  $C_{m-s}$  is the carrier power level available at the sending station, when the master is transmitting. The term  $C_{s-s} - C_{m-s}$  represents the sending station up-link attenuation, which exceeds the up-power control compensation range.

In figure 8 the number of bits to inspect, in order to get an  $E_b/N_0$  with a 99.5% confidence interval of 0.5 dB, is given for the signal magnitude thresholds of 5/8 and 6/8 respectively. The choice of the threshold depends on the link quality dissemination method employed. In the case of the direct method the range of  $E_b/N_0$  is 7-12 dB, so the best value of the threshold is 5/8. Using the indirect method the quality of the RB must be determined by all the stations, resulting in a wider range. In fact the RB is always sent at 2Mbit/s to allow a margin for the faded stations and  $C/N_0$  is 6 dB higher. The resulting range of 7-18 dB implies that the 6/8 threshold should be chosen.

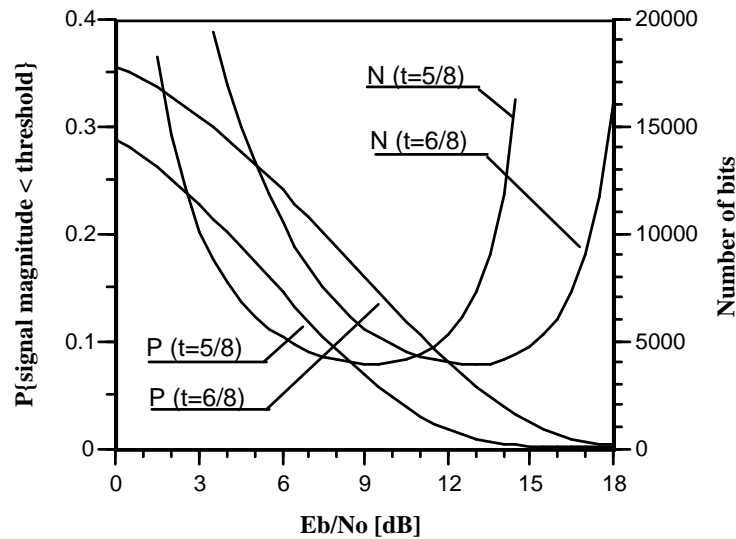


Figure 8: Probability that the signal magnitude is less than the threshold  $t$  and number of bits for an  $E_b/N_0$  estimation with a 99.5% confidence interval of 0.5 dB versus  $E_b/N_0$ .

## 2.4 System performance in fade conditions

The best way to show the performance of a fade countermeasure system is to show how much the system is able to improve the outage probability of a link, i. e. the probability (denoted here by  $P_O$ ) that the BER over a link is higher than the target value. The complexity involved in deriving  $P_O$  in closed form is due to the huge number of the possible system states. In fact, each station can be in one of the  $f$  possible fade levels. So the number of the mutually exclusive states in which the system can be, for  $n$  stations, is  $f^n$ , where  $f$  is a number between 6 and 10 (depending on the considered COS). The number of the system states is thus prohibitively high, even for a small  $n$ .

A Monte Carlo analysis has thus been developed to investigate the  $P_O$  variation on the amount of the common resource and/or on the compression factor of the application bandwidth. The simulation program, written in C, runs on an IBM RISC 6000 machine. The CPU cost of the entire analysis was roughly of 300 hours.

For each  $P_O$  estimation a sample of 1000 favourable events was collected, thus getting a 99.5% confidence interval of  $\pm 10\%$  for the mean value. The cumulative attenuation distributions of the stations are computed using the CCIR interpolation formula<sup>9</sup>:

$$A_p = A_{0.01} 0.12 p^{-(0.546 - 0.0043 \log p)}$$

where  $A_p$  is the attenuation in dB exceeded for a  $p$  percentage of the time and  $A_{0.01}$  is the attenuation exceeded for 0.01% of the time.

All the tests were made for stations of intermediate climatic characteristics inside the Italian region. For these sites, the  $A_{0.01}$  parameter at 11.6 GHz is available thanks to five years data of the Sirio experiment at the Telespazio Fucino station<sup>12</sup>. The  $A_{0.01}$  parameter used in the simulation experiments has been obtained by frequency scaling these experimental results. In addition, some tests were made for stations like Lario ( $A_{0.01}$  still derived from Sirio), a site particularly heavy faded in the north of Italy. In Tab. 3 the parameters  $A_{0.01}$  used for the simulation are reported, for both types of stations and for both up and down-link frequencies, respectively.

Frequency [GHz]	A <sub>001</sub> [dB] Fucino-like stations	A <sub>001</sub> [dB] Lario-like stations
30	22.5	59
20	12	29

Table3: Attenuation exceeded for 0,01% of the time (A<sub>001</sub>) for Fucino and Lario-like stations. Data frequency scaled from the 11.6 GHz values of the SIRIO experiment.

The statistical dependence of the attenuation experienced by the stations has been taken into account by introducing a factor  $h$ , according to the model adopted by Carassa<sup>13</sup>. Denoting the probability to exceed a certain attenuation at each station by  $P_A$ , the joint probability  $P_{A_j}$  to exceed that attenuation at  $n$  stations is

$$P_{A_j} = h^{n-1} P_A^n$$

A value of  $h = 1$  simulates the statistical independence among the attenuations of the stations, while a value of  $h = 20$  has been considered as the maximum station dependence. This value of  $h$  was measured between two stations rather close together<sup>12</sup> (Lario and Spino d'Adda, 85 Km apart) and with very similar climatic characteristics.

The following assumptions were made in order to simplify the Monte Carlo simulation:

- all the stations have the same cumulative attenuation distribution;
- all the stations have the same performance in terms of EIRP, G/T and the same geometric position with respect to the satellite;
- each station sends data over only one point-to-point link with one of the other stations;
- all the links have the same capacity;
- the factor  $h$  is assumed the same for all the stations;
- only stream type links with guaranteed bandwidth are considered in the  $P_O$  evaluation;
- the datagram capacity is seen as a common resource to be shared among the stream links, when faded, in the percentage indicated in the graphs. No investigation has been made on the available datagram capacity in order to evaluate the datagram links outage probability.
- no transponder intermodulation noise reduction, due to one attenuated carrier, is taken into account;
- data reported in Tab. 2 were assumed as the link budget parameters.

The FODA/IBEA system implements both the UPC and the VBCR features. Comparisons are made with systems without UPC and/or without VBCR. Systems without VBCR are assumed to send permanently redundant data, in such a way as to occupy a bandwidth equivalent to the sum of the stream plus the common resource bandwidth occupied by the systems working with VBCR. It must be emphasized that the common resource used by FODA/IBEA is available for datagram traffic (as shown later on) for most of the time, while a system without VBCR has no space available for datagram, even under low fade conditions.

The minimum  $E_b/N_0$  net value is fixed at 6 dB because, for lower values, the modem burst acquisition performance is poor. This poses a limitation on the utilized coding rates. In fact, even for the  $COS = 0$ , the minimum usable coding rate is 2/3. The comparison with systems without VBCR was made by considering the coding rates: 7/8, 4/5, 3/4 and 2/3, with redundancy from 1.14 to 1.5 respectively. For higher redundancy (e. g. 2, equivalent to 100% of the common resource) a

suitable redundancy was introduced on the bit rate of both the preamble and the data. The sum of the contributions given by the UPC, the coding gain and the bit rate redundancy was taken into account as an increment of the link budget margin (LBM). The simulation program was run with equivalent LBM values and no common resource to obtain  $P_O$  relative to systems without VBCR.

In the simulation the transponder is employed without automatic gain control (AGC) and the up-link C/No of 84.2 dB is relative to a transponder gain close to the minimum. The LBM reported in Tab. 2 is 1 dB; this value is assumed in all the simulation runs, unless different values are expressly indicated. In order to increase LBM in the present environment, it is necessary to increase the up-link C/No by reducing the satellite input back-off. This fact may force us to reduce the number of carriers on the transponder.

## 2.5 Simulation results

In Tab. 4 a summary of the most significant parameters relevant to the various simulations is reported. All of the simulations were made for the  $h$  parameter equal to 1, 5 and 20, respectively. Large scale irregularities in the graphs are due to the threshold effects produced by the discrete nature of the COS tables. Small scale irregularities are due to the confidence interval  $\pm 10\%$ .

Depending upon the number of stations, different aspects of the system performance are shown.

Runs with 48 stations were made considering 64 Kbit/s links with  $COS = 0$ . In Fig. 9  $P_O$  is reported, for Fucino-like stations, as a function of the amount of the used common resource and the station dependence factor. Four systems are compared with all the combinations of the UPC and VBCR features. It is evident that the full FCM system needs only 50% of the common resource to give the maximum improvement of  $P_O$ , while the same system without UPC would need a common resource greater than the allowable one to reach the maximum gain. This tendency is even more obvious in the case of Lario-like stations (Fig. 10). As expected, the dependence of  $P_O$  on the factor  $h$  is higher if the common resource is smaller. In Fig. 12 the probability that a certain percentage of the common resource is exceeded is reported for the two types of stations.

Number of stations	link capacity [Kbit/s]	total stream capacity [Kbit/s]	capacity for datagram [Kbit/s]	system overhead <sup>(*)</sup> [Kbit/s]
48	64	3072	3326	1794
10	384	3840	3858	494
2	1920	3840	4131	221

Table 4. - Simulation parameters. Channel capacity = 8192 Kbit/s

In Fig. 11  $P_O$  is reported, for Fucino-like stations, as function of LBM, for an availability of 50% of the common resource. This graph allows an evaluation of how big the LBM must be, once a certain  $P_O$  is required. The comparison among the four systems is straightforward. For a  $P_O$  of  $10^{-4}$  the UPC+VBCR system gains about 10 dB on the UPC system and 18 dB on the system without any FCM. The comparison with the VBCR system would be more fair only allowing a higher amount of the common resource.

For the 10 and the two stations runs (Figs. 13-15), H.261 videoconference applications are considered, with  $COS = 1$  (high quality video) and rates of 384 and 1920 Kbit/s, respectively. Such applications are supposed to be compressible in bandwidth, for the VBCR systems, by a factor

(\*) reference burst + two control slots + stream slot preamble + control sub-burst



between 1 and 6 in the 384 Kbit/s case and by a factor between 1 and 15 in the 1920 Kbit/s case, respectively. The results of these runs are reported in Figs. 16 to 18. In general it can be seen that by increasing the compression factor of the applications the common resource occupancy is saved for a higher percentage of the time. In fact, for a certain compression factor the gain increases only up to a certain percentage of the common resource occupancy. Conversely the graphs allow an evaluation of the percentage of time during which the application is compressed at the various levels, once the percentage of the common resource made available is fixed.

## Conclusions

A flexible TDMA station has been implemented. With its associated modem it allows very complex and efficient TDMA systems to be designed. Of particular importance is the system's ability to transmit data packets with multiple data and coding rates. This allows the information bit energy of each packet to be tailored to the prevailing conditions at the required grade of service. The TDMA system can be used to implement a complex system based on the FODA/IBEA architecture. This allows both stream and packet traffic to be accommodated in the same network. In addition stations can operate with reduced power margins since the system adapts the transmitted bit energy in real time to counteract fade conditions. Such a system will allow the use of smaller earth stations and so will improve the economics of user-located satellite communications networks.

The system performance analysis has been made using a Monte Carlo simulation. This study shows that, using the FODA/IBEA system, the outage probability of a link can be reduced to acceptable values even in Ka band, when transponders with good performances (i.e. with spot coverages), such as Olympus, are employed. The common resource, i.e. the capacity allocated for datagram is scarcely used by the faded stream links. The analysis of the system has been made for the stationary case. Further studies will investigate the speed of the system reaction to dynamic changes of the fade conditions.

## Acknowledgements

The authors wish to thank Mr. A. Baslington, Mr. A. brown, Mr. M. Williams and Mr. R. Wilden from Marconi R.C. (U.K.), Mr. A. Marzoli and Mr. M. Neri from Telespazio (I) for their precious collaboration.

## References

1. Celandroni N., Ferro E., Marzoli A.  
"Fade detection in the FODA system", proceedings of the Olympus Utilization Conference, Vienna (A), 12-14 April 1989.
2. Celandroni N., Ferro E.  
"Voice/data integrated transmission on a variable bit and coding rates satellite link", proceedings of the SICON '89 Singapore International Conference on Networks, pp. 449-453, July 1989, Singapore.
3. Celandroni N.  
"Estimation of the Eb/No ratio using PSK quantized levels in an additive white gaussian noise (AWGN) environment", CNUCE Report C90-22, September 1990.
4. Celandroni N., Ferro E., Dossi L., Tartara G.  
"User oriented satellite networks: studies on the utilization of transmission capacity in TDMA

- and TDMA/FDMA systems", European Transactions on Telecommunications, Vol. 2. N. 4, July-August 1990.
5. Celandroni N., Ferro E.  
"The FODA-TDMA satellite access scheme: presentation, study of the system and results", IEEE Transaction on Communication, V. 39, N. 12, pp.1823-1831, December 1991.
  6. Celandroni N., Ferro E., Potorti F., Mihal V.  
"The FODA/IBEA satellite access scheme. System description", CNUCE Report C92-05.
  7. Eluzor Friedman  
"Packet voice Communications over PC-Based Local Area Networks", IEEE Journal on Selected Areas in Communications, Vol. 7, N. 2, February 1989.
  8. Holt A.R., Mc. Guinness R., Evans B.G.  
"Frequency scaling propagation parameters using dual-polarization radar results", Radio Sci., Vol. 19, pp. 222-230.
  9. CCIR [1990] Report 564-4  
"Propagation data and prediction methods required for earth-space telecommunication systems".
  10. Shuzo Kato, Masahiro Morikura, Shuji Kubota, Hiroshi Kazama, Kiyoshi Enomoto:  
"A TDMA satellite communication system for ISDN services -Offset QPSK burst modem coupled with high coding gain FEC-", proceedings of GLOBECOM '91, Phoenix (USA), November 1991.
  11. Capsoni C., Matricciani E., Mauri M., Paraboni A.:  
Il "Frequency Scaling" - Programma Sirio - I principali risultati dell'esperimento di propagazione di onde elettromagnetiche a frequenza superiore ai 10 GHz. Vol II pp. 117-156. CNR-CSTS - Roma, 1983.
  12. Carassa F., Matricciani E., Tartara G.:  
"Frequency diversity and its applications", International Journal of Satellite Communications, Vol. 6 N. 3, pg. 313-322, July-September 1988.
  13. Carassa F.:  
"Technical aspects in the future development of satellite communication systems with particular reference to the use of frequencies above 10 GHz', proceedings of the 19th Int. Conf. 'Scientifico sullo spazio', Rome, March 1979, pp. 22-41.
  14. Olympus Users' Guide UG-6-1 Part 4:  
"20/30 GHz Communication Payload", CCB/52182/HHF/CMM, Issue 3, February 1988.
  15. In orbit test results of the recovered Olympus satellite, TE/56203/CM/ap, Issue 1, September 1991.

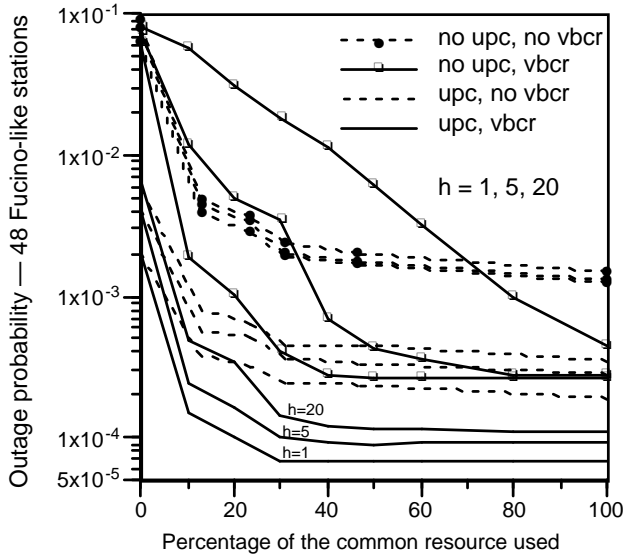


Figure 9: Four systems are compared: with and without VBCR, with and without UPC. 48 Fucino-like stations are considered.

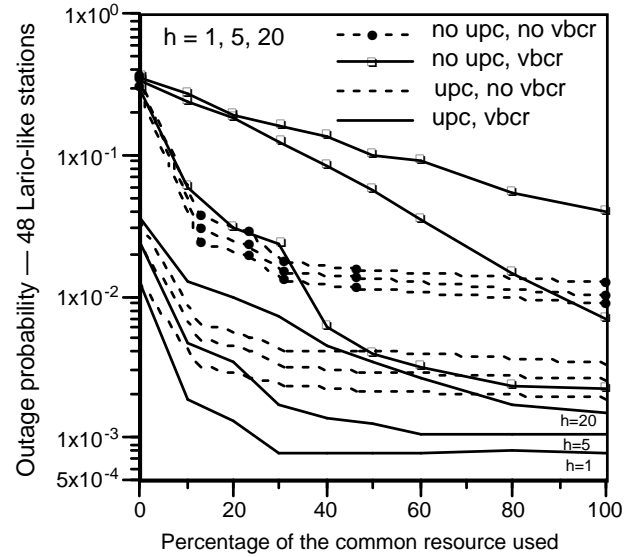


Figure 10: Four systems are compared: with and without VBCR, with and without UPC. 48 Lario-like stations are considered.

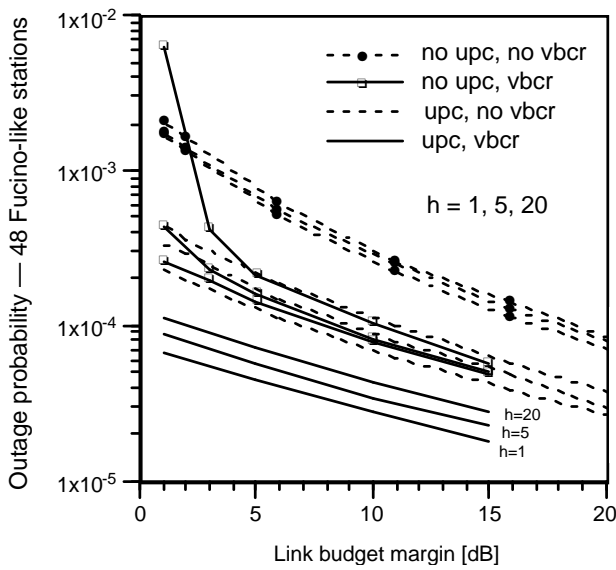


Figure 11: Four systems are compared: with and without VBCR, with and without UPC. 48 Fucino-like stations are considered.

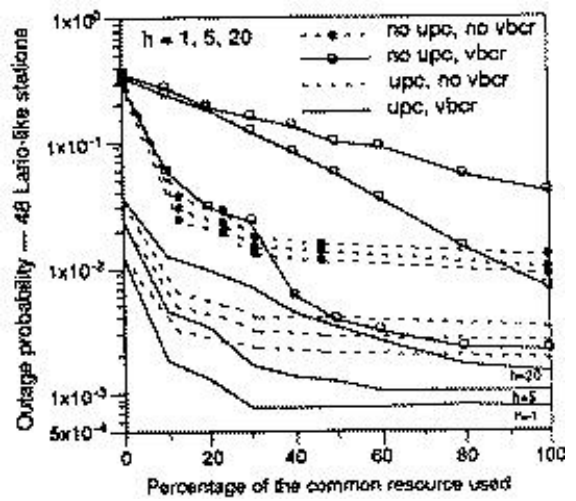


Figure 12: Four systems are compared: with and without VBCR, with and without UPC. 48 Fucino-like stations are considered. The used common resource was 50% of the available one.

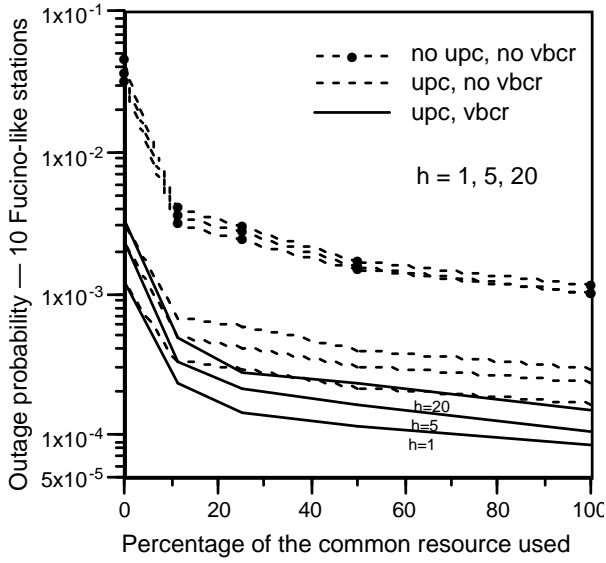


Figure 13: The FODA/IBEA system is compared with two systems with fixed bit and coding rate, one of them with up power control. 10 Fucino-like stations are considered.

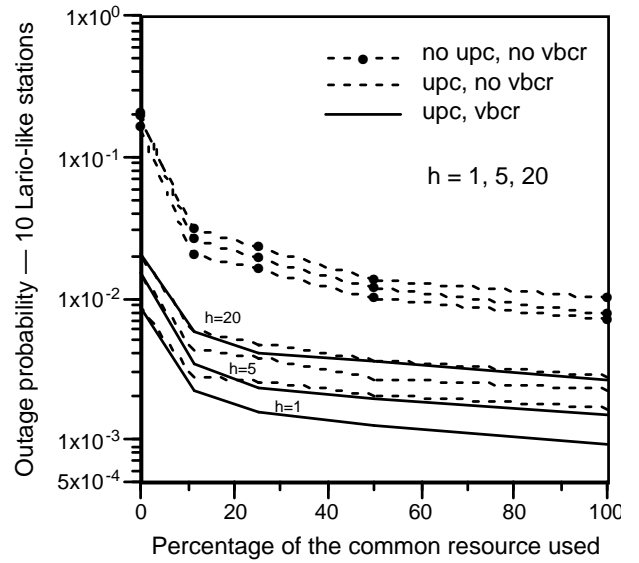


Figure 14: The FODA/IBEA system is compared with two systems with fixed bit and coding rate, one of them with up power control. 10 Lario-like stations are considered.

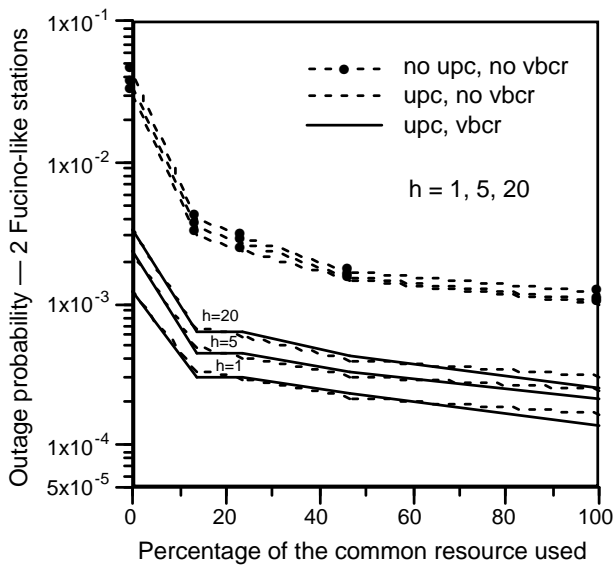


Figure 15: The FODA/IBEA system is compared with two systems with fixed bit and coding rate, one of them with up power control. Two Fucino-like stations are considered.

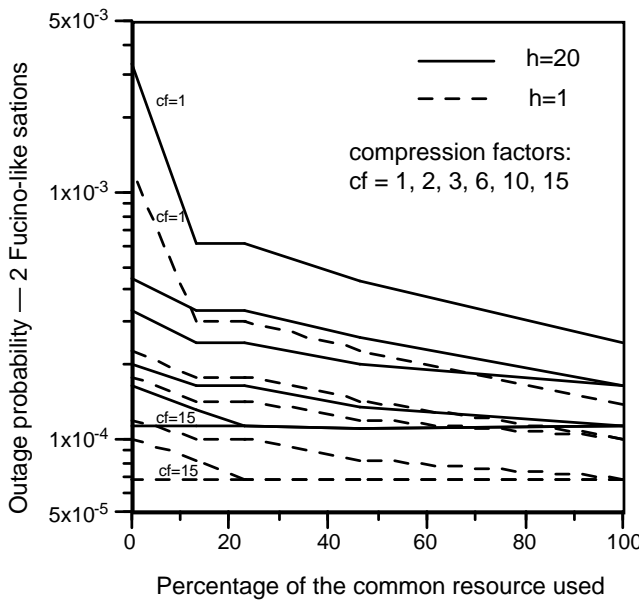


Figure 16: Performance of the FODA/IBEA system loaded with applications allowing different compression factors. Two Fucino-like stations are considered.

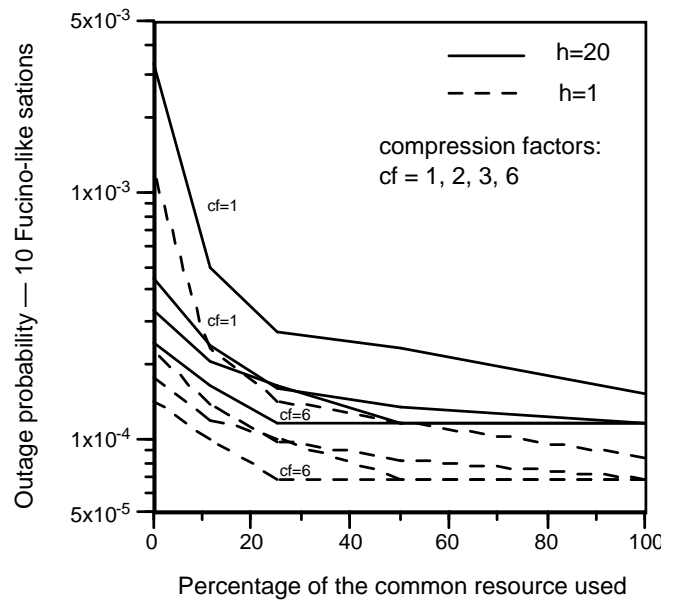


Figure 17: Performance of the FODA/IBEA system loaded with application allowing different compression factors. 10 Fucino-like stations are considered.

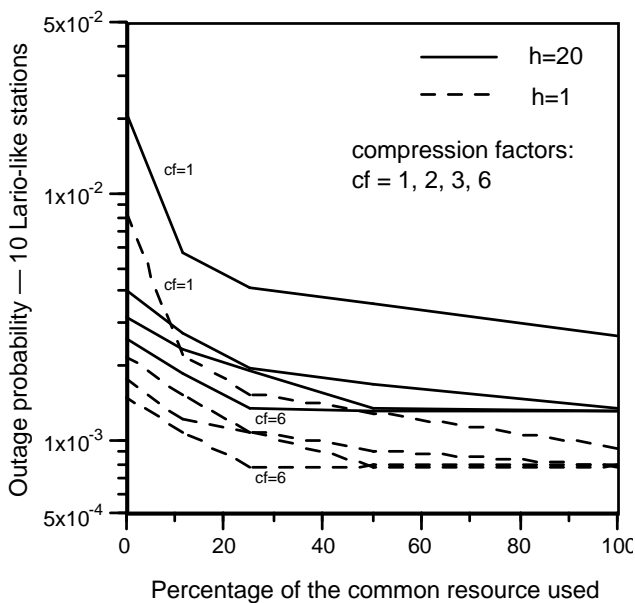


Figure 18: Performance of the FODA/IBEA system loaded with applications allowing different compression factors. 10 Lario-like stations are considered.